

JOURNAL OF CIVIL ENGINEERING FRONTIERS

www.jocivilef.org

An Investigation of Liquefaction Potential and Risk for Seismic Zonation in the Saqqez Region of Kurdistan, Iran

Semko Arefpanah^{1,*}, Alireza Sharafi², Bavandi Omid³

¹ Department of Civil Engineering, Science and Research Branch₂Islamic Azad University, Tehran, Iran Semko.arefpanah@srbiau.ac.ir

²Department of Civil Engineering, Science and Research Branch₂Islamic Azad University, Tehran, Iran Alireza.sharafi@srbiau.ac.ir

³Department of Civil Engineering, Qaemshahr Branch Islamic Azad University, Mazandran, Iran Bavandi68@gmail.com

Abstract

Liquefaction occurs in loose sandy or fine-grained soils. This phenomenon leads to symmetric or asymmetric settlement, reduced bearing capacity of shallow foundations and piles under loads, and increased lateral forces required for structural protection. During earthquakes, liquefaction can damage human infrastructure and alter the surface geomorphology. Identifying liquefaction-prone areas is critical to mitigating the destructive effects of this phenomenon. This identification can be achieved through zoning, where the risk tolerance of different locations is evaluated. Zoning of liquefaction-prone areas significantly reduces earthquake-induced damages. This article presents research findings on zoning the liquefaction potential in Saqqez City. The zoning is conducted in accordance with the guidelines outlined in the Geotechnical Earthquake Engineering Guidelines and Seismic Hazard Zoning. The results indicate that the Saqqez City River is generally classified into two zones Liquefaction likely and not likely regarding liquefaction risk in the event of a future earthquake. The objective of this article is to elucidate the methodology for seismic hazard zoning in Saqqez City based on influencing factors.

Keywords: Liquefaction, Geomorphology, Geology, Iran, Seismic Zonation.

Received: February 06, 2025 / Accepted: March 22, 2025 / Online: April 3, 2025

I. INTRODUCTION

Iran, situated within the seismically active Alpine-Himalayan orogenic belt, experiences frequent and severe earthquakes, posing a significant threat throughout the country. The recurring devastation underscores the necessity of proactive seismic hazard mitigation planning because of the substantial potential for human casualties and economic losses. Earthquakes, as natural hazards, are a critical concern in societal development, with their associated damage and impact on community resilience steadily increasing [1].

A key seismic hazard is the potential for geotechnical failures, particularly those induced by strong ground motion. These failures, contingent on both structural conditions and earthquake characteristics, can result in ground deformation and structural damage. Liquefaction is a critical geotechnical hazard, occurring in saturated, loose sandy to silty soils. Seismic loading on these susceptible soils causes a tendency for volume reduction, while the inability of pore water to dissipate rapidly leads to increased pore water pressure and reduced effective stress, ultimately diminishing soil resistance. This process can result in the soil exhibiting fluid-like behavior, a phenomenon known as liquefaction. Post-earthquake,

liquefaction can exacerbate the initial seismic damage, posing ongoing risks. Consequences of liquefaction include damage to lifelines, excessive settlement and tilting of structures, flotation of buried utilities, well contamination, and morphotectonic changes.

Several studies have investigated liquefaction potential in Iran. Orang assessed the liquefaction susceptibility of sandy soils in the Babolsar region [2]. Orang (1995) suggested that a 4 km wide coastal strip during earthquakes with a 500-year return period [3]. Conducted detailed studies in Tehran, identifying the southern regions as having significant liquefaction potential [4]. These studies often considered natural criteria such as slope, faults, and lithology, as well as physical criteria like structural density, land use, and social factors. Following the 1997 Niigata earthquake, liquefaction vulnerability zoning became a priority [5].

Iran's tectonic setting within the Alpine-Himalayan belt contributes to its high seismic potential [6]. Researchers like Yamamoto have developed regional hazard maps for cities like Tokyo and San Francisco [7]. Turkey, another seismically vulnerable country, has a

paruinta www.ipacademia.or.

significant portion of its population and GDP located in high-risk zones. Various researchers have employed remote sensing, GIS, and spatial analysis to assess seismic risk and vulnerability in Iranian cities, including Tabriz; [8], [9], Sanandaj [10], Zanjan [11]), Sabzevar [12], and Qazvin [13]. Studies have also addressed broader aspects of seismic risk, including social vulnerability [14], physical vulnerability [15], and the impact of natural hazards on environmental conditions [16]. Zoning studies in Iran were initiated after the Manjil earthquake by the International Institute of Seismology and Earthquake Engineering [17] categorized geographic areas based on their response to natural disasters.

This current study is part of a broader investigation of seismicity and geotechnical earthquake engineering in Kurdistan province. This article summarizes previous related research. Liquefaction zoning is being conducted at three levels. This article focuses on the first and second levels of zoning and their application to the present research, utilizing available data to assess liquefaction risk throughout Kurdistan province.

II. LIQUEFACTION RISK ZONING

A. Soil Liquefaction and Level 1 Zonation

Soil liquefaction, a phenomenon causing structural instability, settlement, reduced bearing capacity, and increased lateral forces, has been studied extensively since the 1964 Niigata earthquake. Assessment methods, integrated into international standards, utilize historical earthquake data, geological conditions, groundwater levels, and geotechnical properties.

Level 1 zonation maps, the fastest and most basic evaluation tool, provide a preliminary estimate of liquefaction risk. They rely on existing data, historical records, and regional geological/geomorphological features, typically scaled between 1:1,000,000 and 1:50,000. These maps classify hazard levels and identify vulnerable areas but require supplementary methods for comprehensive analysis.

-Key Features of Level 1 Zonation:

Rapid, initial risk assessment.

Based on accessible data, reports, and geological structure. Classifies hazards and prioritizes zones for further study.

Highlights variable risk levels across regions.

B. Determining the Maximum Size of the Area Susceptible to Liquefaction

Historical data allows us to assess the risk ratio of the target area, considering fault activity and active earthquakes. The morphotectonic risk can be directly derived from earthquake predictions. In simpler terms, the extent of liquefaction is determined by the earthquake's epicenter distance and intensity, according to established criteria.

Since liquefaction is a phenomenon that may occur repeatedly in one place, If the underground water level and the physical conditions of the deposits (specific gravity, etc.) have not changed, by examining studies of past earthquakes in areas that have the potential for liquefaction, it is possible to prepare maps of the possible occurrence of liquefaction [18].

Based on the moment magnitude scales [19] and Wells Coppersmith [20], a linear relationship between Iranian earthquakes of eqs 1 has been developed. In this way, the relationship between magnitude and fault rupture length for Iranian earthquakes is presented as the following relationship: And finally, the average results obtained by these two researchers will be used. Which is in the relationship of L_F (otal mapped length of a fault) and L_R (Length of the fault segment that actually slipped during an earthquake). For hazard assessment, L_R is often estimated from L_F using empirical ratios (e.g., $L_R{\approx}0.37 \cdot L_F$ for strike-slip faults).

$$M_W = 0.91 Ln L_R + 3.66$$
 (1)

C. Determining the Distance of the Farthest Area with Liquefaction Potential to the Earthquake Focus

Earthquake activity in a region can be assessed using historical data, allowing for direct estimation of the prone area based on earthquake magnitude. Many researchers have investigated the distribution of liquefaction areas in past earthquakes, developing formulas relating the distance from the epicenter to the farthest liquefied area (R_m) to the earthquake's magnitude (M_w) . These formulas describe how the farthest distance of liquefaction from the earthquake's center changes with magnitude. For example, authors of [21] proposed a formula based on data from 32 earthquakes in Japan. As [22] notes, the distance beyond which liquefaction is unlikely can be determined by plotting the epicentral distance against earthquake magnitude for sites known to have liquefied.

$$\log R = 0.77 M_w - 3.6 \tag{2}$$

The earthquake magnitude (M_w) used in the Koribayashi and Tatsuoka formula is based on the Japan Meteorological Agency's definition. (R_m) represents the farthest distance from the seismic zone to the epicenter, measured in kilometers.

In Figure 1 helps engineers and geologists assess the likelihood of soil liquefaction based on the SPT blow count (\overline{N}) and the effective overburden stress $(\sigma_{\mbox{\tiny o}}').$ By plotting these values on the graph, one can determine whether a particular soil condition falls within the liquefaction-prone zone (black circles) or outside it (white circles). The various curves provide guidelines for different soil types and conditions, aiding in the design of structures and foundations in areas susceptible to liquefaction.

 \overline{N} (on the x-axis): represents the Standard Penetration Test (SPT) blow count, which is a measure of the density

and strength of the soil. Higher N values indicate denser and stronger soil.

 σ_{\circ} ' (on the y-axis): This represents the effective overburden stress, which is the pressure exerted by the weight of the soil above a given point. It is typically measured in units of stress, such as kilopascals (kPa).

There are two types of data points:

Black circles: These represent cases where liquefaction occurred.

White circles: These represent cases where liquefaction did not occur.

Several curves are plotted on the graph, representing different criteria or models for predicting liquefaction potential. These include:

Seed et al., 1984: A set of curves that define boundaries for liquefaction potential based on research by Seed and colleagues [22].

Ambraeys, 1988: Another set of curves providing additional boundaries for liquefaction. The curves are labeled with values such as $\log e_a = 1.0$, 1.5, etc., which likely refer to logarithmic values of some parameter related to energy or strain.

The graph distinguishes between different types of soil:

Clean sands: Soils with minimal fines content.

Sands, 15% fines: Soils containing a higher percentage of fines (smaller particles).

Shaded Region: There is a shaded region in the middle of the graph, which may represent a zone of uncertainty or a transition area between liquefied and non-liquefied conditions.

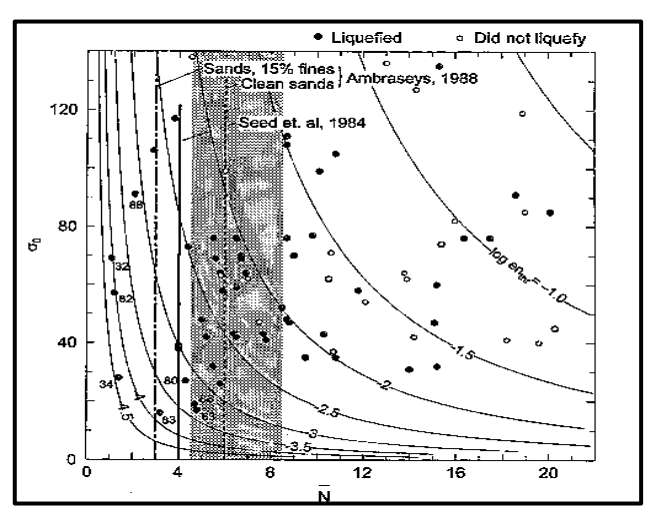


Fig. 1. Contour Plot of σ_0 vs. \overline{N} with Cutoff Criteria and en thr Levels.

Figure 1 presents a plot of σ_0 (distance) versus \overline{N} (magnitude) for the combined dataset. The data points are represented by symbols, while contours of equal "en thr" values are shown. These contours are spaced logarithmically, with eight values ranging from LOG10 (ENTHE) = -1 to 4.5. The figure also includes heavy vertical lines at $\overline{N}=3$, 4, and 6. Finally, shaded regions

indicate the cutoff distance criteria proposed by Seed et al. and Ambraseys.

Synthesized existing data on liquefaction, including work by Kuribayashi and Tatsuoka, Youd, Davis, and Berrill, and additional Japanese data on liquefaction from after 1975. Based on this comprehensive dataset, they proposed a formula to estimate Rm is in kilometers (epicentral), which represents a characteristic distance related to liquefaction potential [23].

This is represented by a set of curves labeled "N=4."

$$\log R = 0.463 M_{\rm w} - 1.14 \to \overline{N}4 \tag{3}$$

In their 1984 study, Liu and Xie compiled comprehensive global earthquake data and proposed the following formula for calculating seismic magnitude, where M_L represents the local magnitude on the Richter scale [24].

$$R = 0.82 \times 10^{0.862(M_L - 5)} \tag{4}$$

Criteria have been developed to evaluate the likelihood of liquefaction at a site influenced by the seismic energy generated by earthquakes. Based on this framework, four deterministic criteria have been derived to analyze the relationship between earthquake magnitude, distance from the seismic source, and the threshold energy required to trigger soil liquefaction. By integrating seismic and geotechnical parameters, these criteria establish boundaries beyond which seismic events are deemed negligible in terms of their potential to induce liquefaction at the site. This approach enables engineers to optimize their analyses by focusing on events with sufficient energy to provoke liquefaction.

The significance of these four criteria lies in their ability to reduce uncertainties and enhance the precision of liquefaction hazard assessments. By defining energy thresholds based on magnitude and distance, the deterministic criteria act as a filter to eliminate low-impact or distant seismic events. This streamlines computational efforts, saving time and resources, while prioritizing critical scenarios. Furthermore, these criteria account for intrinsic soil properties (e.g., shear strength, moisture content) and seismic conditions to inform mitigative measures such as soil improvement or deep foundation systems. Ultimately, this analytical framework serves as a practical tool in seismic geotechnical engineering, improving structural safety in liquefaction-prone areas.

The critical maximum distance, R (expressed in kilometers), is the farthest distance at which liquefaction is first observed. It is widely accepted that liquefaction does not occur beyond this distance unless the site is "exceptionally soft" (e.g., shallow water-saturated Holocene deposits). Equation (3) assigns R to locations prone to liquefaction. Figure 2 illustrates the distance cutoff criterion, described by Equations (7) (bold solid and dashed lines). A significant discrepancy is observed

between R_m estimates from Equations (6–7) for M=5: Tinsley et al. suggest $R_m \approx 1$ km, whereas Seed et al. propose $R_m \approx 15$ km. This disparity diminishes with increasing magnitude (from ~15-fold at M=5 to ~2-fold at M=7.5).

The uncertainty in R_m estimation stems from insufficient comprehensive field observations and the multitude of factors influencing field liquefaction susceptibility, including particle size distribution, initial relative density, effective initial stress, excitation amplitude, load duration, overburden shear resistance, drainage, soil compressibility, layer thickness, and others. Consequently, R_m estimates should be periodically revised as additional data become available [25].

In Figure 2 is used to compare and visualize the empirical relationships between earthquake magnitude and distance as proposed by different studies. Each line or curve corresponds to a specific formula, allowing researchers and practitioners to estimate distances based on observed magnitudes or vice versa. The varying slopes and intercepts of the lines reflect the differences in the underlying assumptions and data used in each study.

In Figure 2, according to research Ambreys two equations are given:

$$M_W = -0.31 + 2.65 \times 10^{-8} R_M + 0.99 \log R_M$$
 (5)

$$M_W = 0.18 + 9.2 \times 10^{-8} R_{FM} + 0.90 log R_{FM}$$
 (6)

Here, $R_{\rm m}$ is in centimeters (epicentral), and $R_{\rm fm}$ is in centimeters (distance to the fault).

Tinsley et al., 1985: provided a formula where R is in kilometers. The curves show how the distance (R) varies with magnitude (M) according to each model.

$$Log R = \begin{cases} 0.856(M-5), M < 7.5\\ 2.14, M > 7.5 \end{cases}$$
 (7)

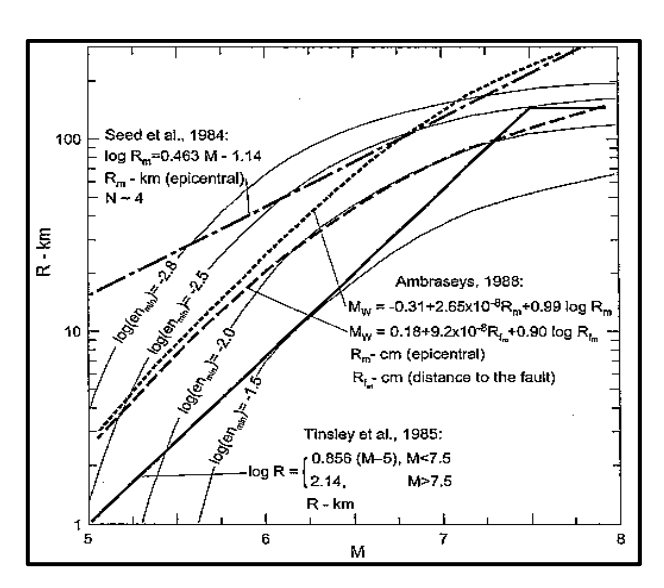


Fig. 2. Magnitude-Distance Cutoff Criteria Based on Threshold Energy and Liquefaction Distance.

Figure 2 magnitude-distance cut-off criteria defined by equations (1-11) four cut-off criteria derived via the threshold energy to liquefy a site also analyzed earthquake data and developed a formula relating earthquake magnitude to liquefaction distance for shallow and medium-depth earthquakes. In this formula, (Rm) represents the horizontal distance between the fault causing the earthquake and the farthest point of liquefaction [26].

$$\log R = 0.88 M_{\rm w} - 4.4 \tag{8}$$

Authors of [27] reviewed the 1975 research of Kuribayashi and Tatsuoka. Incorporating new data from 67 earthquakes spanning 106 years, Wakamatsu established a revised upper bound for the relationship between R and (M_j) for $M_j > 5$. This update refined the original formula proposed by Kuribayashi and Tatsuoka (1975).

$$\log R = 2.22\log (4.22M_w - 19) \tag{9}$$

Authors of research [28] also proposed the following formula by considering the data related to important seism dynamics.

$$\log R = 3.5\log (1.4M_w - 6) \tag{10}$$

D. Severity Criteria

Studies conducted by Korybayshi, Tatsuoka, and Wakamatsu indicate that soil liquefaction in loose, young Holocene deposits (formed within the last 11,700 years) typically occurs during earthquakes with intensities exceeding JMA (Japan Meteorological Agency) scale degree V or Modified Mercalli Intensity (MMI) VIII. However, even at lower intensities, such as JMA scale degree IV, mild liquefaction may occur, which should not be overlooked in seismic hazard assessments. These deposits, due to their water saturation and loose structure, are more vulnerable to liquefaction compared to older soils like Pleistocene deposits. These degrees according to earthquake severity are shown in Table 1 for before 1991.

The findings of this research are critical for earthquake engineering and structural design in seismically active regions, as they underscore the necessity of employing soil reinforcement methods (e.g., dynamic compaction or pile driving) and adhering to international standards (such as United Nations documents, likely referencing UN 1982 or 1987). Ignoring these intensity thresholds could lead to land subsidence, structural collapse, or irreparable damage.

TABLE1 J.M.A INTENSITY (BEFORE 1996)

Classification	Measured Intensity
0	0-0.4
I	0.5-1.4
II	1.5-2.4
III	2.5-3.4
IV	3.4-4.4
V lower	4.5-4.9
V upper	5-5.4
VI lower	5.5-5.9
VI upper	6-6.4
VII	> 6.5

E. Liquefaction Potential of the Investigated Area Based on Available Information

E.1. Based On the Criteria of Geology and Geomorphology

Liquefaction recurrence is a geotechnical hazard that can manifest repeatedly in susceptible regions under cyclic seismic loading. Historical liquefaction manifestation maps, derived from post-event investigations of prior earthquakes (e.g., seismic events in Japan), serve as critical tools for identifying zones with heightened liquefaction potential during future seismic activity. By correlating historical liquefaction occurrences with the geologic and geomorphic characteristics of affected areas—including soil stratigraphy, groundwater table depth, and depositional environment—engineers can delineate regions with analogous susceptibility profiles.

Authors of [29] developed an empirical classification system for liquefaction susceptibility through statistical analysis of extensive Japanese earthquake datasets, integrating parameters such as soil type, SPT (Standard Penetration Test) values, and seismic intensity. This framework, summarized in Table 4, enables preliminary liquefaction potential assessment by categorizing geologic units based on their propensity for pore pressure generation and shear strength degradation under dynamic loading. The methodology aligns with ASCE/SEI 7-22 provisions for seismic risk evaluation and Eurocode guidelines for liquefaction hazard zonation, providing a foundational approach for site-specific geotechnical investigations.

E.2. Using the Liquefaction Severity Index (LSI)

The idea of an "index LSI" was defined in terms of the distance from the seismic energy source in order to quantitatively quantify the intensity of the impacts of liquefaction. This index, which is offered for riverine and deltaic deposits with a gentle slope that are prone to erosion and geologically belong to the last Holocene, represents the maximum change in the horizontal location of the earth due to lateral expansion in liquefaction.

F. Second-Class Zoning (Micro zonation).

Utilizing additional information resources in the Kurdistan region, as shown in Figure 3, can significantly

improve the first-class zoning standards. These information resources often include existing geotechnical reports, data on groundwater levels and their seasonal variations, and precise criteria for geology and geomorphology (Table 2-3).



Fig. 3. Location map of the study area (Saqqez City) at national, provincial, and city levels

titled Susceptibility of 2, Detailed Geomorphological Units to Liquefaction Subjected to the Ground Motion of the J.M.A. Intensity V or M.M.S. VIII, and categorizes various geomorphological units based on their susceptibility to liquefaction under specific ground motion conditions. The table is divided into three main columns: Classification, Specific Conditions, and Liquefaction Potential. The table systematically evaluates the risk of liquefaction across various geomorphological units under specified ground motion conditions. It highlights those certain conditions, such as the presence of sandy soil or specific gradients, can significantly increase the likelihood of liquefaction. Conversely, units with gravel or cobble compositions are less susceptible. This information is crucial for assessing and mitigating seismic risks in different geological settings.

Table 3, titled "Susceptibility to Liquefaction of Geomorphological Units, and categorizes different types of geomorphological units based on their likelihood of experiencing liquefaction during seismic events. The table is divided into three ranks (A, B, and C) with corresponding descriptions of the geomorphological units and their associated liquefaction potential.

This classification helps in assessing the vulnerability of different landscapes to liquefaction, which is crucial for urban planning, construction, and disaster preparedness in seismically active regions.

TABLE 2. SUSCEPTIBILITY OF DETAILED GEOMORPHOLOGICAL UNITS TO LIQUEFACTION SUBJECTED TO THE GROUND MOTION OF THE J.M.A. INTENSITY V OR M.M.S. VIII (WAKAMATSU 1992)

Geomorphological Conditions					
Classification	Specific Conditions	Liquefaction Potential			
X7.11 1.1	Valley plain consisting of gravel or cobble	Not Likely			
Valley plain	Valley plain consisting of sandy soil	Possible			
A11 - 1.C	Vertical gradient of more than 0.5 %	Not Likely			
Alluvial fan	Vertical gradient of less than 0.5 %	Possible			
N 11	Top of natural levee	Possible			
Natural levee	Edge of natural levee	Likely			
Back marsh		Possible			
Abandoned river channel	1	Likely			
Former pond	1	Likely			
Marsh and swamp	7	Possible			
Dominion had	Dry river bed consisting of gravel	Not Likely			
Dry river bed	Dry river bed consisting of sandy soil	Possibly			
Delta		Possible			
_	Sand bar	Possible			
Bar	Gravel bar	Not Likely			
-	Top of dune	Not Likely			
Dune	The lower slope of the dune	Likely			
D 1	Beach	Not Likely			
Beach	Artificial beach	Likely			
Inter-levee lowland		Likely			
Reclaimed land by drainage		Possible			
Reclaimed land		Likely			
Spring	7	Likely			
	Fill on the boundary zone between sand and lowland	Likely			
	Fill adjoining cliff	Likely			
Fill	Fill on marsh or swamp	Likely			
	Fill on reclaimed land with drainage	Likely			
	Other type fill	Possible			

TABLE 3. SUSCEPTIBILITY TO LIQUEFACTION OF GEOMORPHOLOGICAL UNITS (IWASAKI 1982)

Rank	Geomorphological units	Liquefaction potential
A	A Present river bed, old river bed, swamp, reclaimed land, and inter-dune lowland	Liquefaction likely
В	B Fan, natural levee, dune, flood plain, beach, and other plains	Liquefaction possibly
С	Terrace, hill, and mountain	Liquefaction not likely

G.Tectonic Summary of the Western Zone of Iran

Regarding Figure 4 An earthquake struck Iran on October 5, 2022, as a result of shallow oblique reverse faulting close to the Iranian-Turkish border. According to focal mechanism solutions, the rupture happened on a reverse fault with a sharp dip to the northeast or a moderate dip to the west-northwest. The earthquake's depth and location suggest that it is an intraplate quake that is taking place within the widely dispersed plate border zone between the Arabian and Eurasian plates, which are convergent. At the site of the earthquake on October 5, the Arabia plate shifts northward in relation to Eurasia, creating the Northern Zagros, Bitlis, and Caucus Mountain ranges and assisting in pushing the Anatolia microplate

Turkey westward into the Aegean Sea .Moderate-magnitude, shallow earthquakes like the one on October 5 are common in Iran, while large (magnitude 7 or greater) ones are relatively rare.

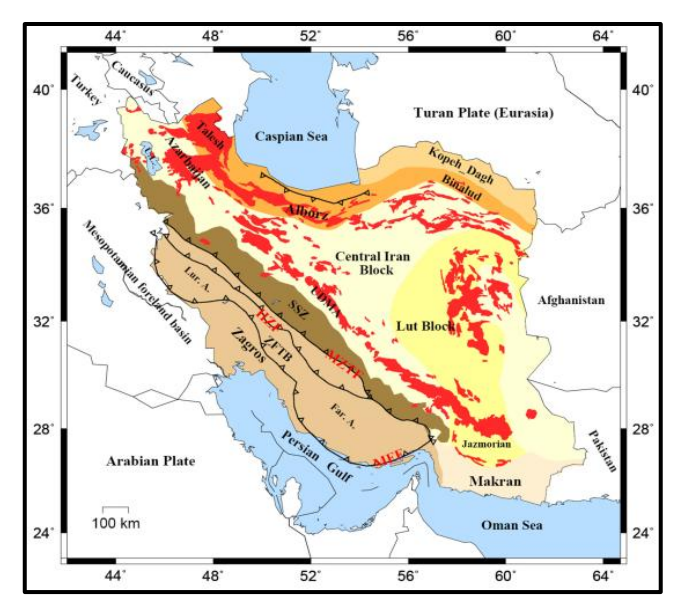


Fig. 4. Tectonic Units of the Iranian Plate.

Figure 4 different tectonic units of the iranian plate. Ul urumieh lake, ssz sanandaj-sirjan zone, zftb zagros fold and thrust belt, mztf main zagros thrust fault, hzf high zagros fault, mff main front fault, udma urumieh—dokhtar magmatic arc, lur. A. Lurestan arc; fars a. Fars arc (jime 2012).

H. Methods Used in the Study Area

The geographical extent of the province lies between 34°44′ to 36°30′ N latitude and 45°31′ to 48°16′ E longitude. Situated on the slopes and scattered plains of the Middle Zagros, the province is bordered by West Azerbaijan and Zanjan to the north; Hamadan and Zanjan to the east; Kermanshah Province to the south; and Iraq to the west. It encompasses nine counties: Sanandaj, Saqqez, Marivan, Baneh, Kamyaran, Bijar, Qorveh, Dehgolan, and Divandarreh.

Kurdistan Province is influenced by two climatic factors: dry summers and cold winters in mountainous regions. A significant portion of the province has a cold, mountainous, and Mediterranean climate with spring rainfall. The climate of Kurdistan plays a crucial role in soil weathering, plant growth, and pasture development, favorable conditions for rain-fed and irrigated wheat cultivation, forest expansion, and horticulture. Due to the mountainous barriers that block moisture-laden western air currents entering the plateau, precipitation decreases from west to east across the province.

Kurdistan Province exhibits two distinct climatic types: a temperate climate with severe winters in mountainous and high-plateau areas, and a milder climate in valleys and western regions. The study area is located within the Sanandaj-Sirjan Zone (Alaei, 2006). The Sanandaj-Sirjan structural zone lies northeast of the Zagros Main Reverse Fault and was first documented by Stocklin in 1968. Fault trends in Kurdistan Province predominantly follow a west-east orientation, with some extending southeast.

According to seismic hazard zonation maps, over 30% of Kurdistan Province—including southwestern and

western regions (Kamyaran, Marivan, Sarvabad, and parts of Divandarreh and Saqqez counties)—faces very high earthquake risk. Nearly 60% of the province, including Sanandaj, Saqqez, Baneh, and Qorveh counties, is classified as high-risk, while remaining areas such as Bijar and Divandarreh are moderate-risk.

The Sanandaj-Sirjan region forms a narrow belt extending between Sirjan and Esfandegh in the southeast and Urmia-Sanandaj in the northwest, eventually merging with the Tauride orogenic belt in Turkey. This region is separated by a narrow (a few kilometers wide) thrust fault. The lithological and structural features of the Sanandaj-Sirjan zone indicate deep basins or rifts within the Precambrian Iranian-Arabian shield, which geologically distinguishes it from neighboring regions, and Figure 5 shows the location of the faults in the Kurdistan region with large earthquake magnitudes in different colors according to their intensity. This zone is approximately 1500 km long and 150 to 250 km wide, extending from the western shores of Lake Urmia in a northwest-southeast direction to the Minab fault and continuing towards Bandar Abbas [31].

Based on recent subdivisions, this belt is categorized into three subzones: the Hamadan-Tabriz Subzone, the Saqqez-Baneh Belt, and the Sanandaj Cretaceous Volcanic Belt. Saqqez city lies within the Saqqez-Baneh Belt, a segment of the Sanandaj-Sirjan Zone located between Nahavand and Urmia. This belt measures 15–20 km in width, 200–300 km in length, and follows a NW-SE trend.

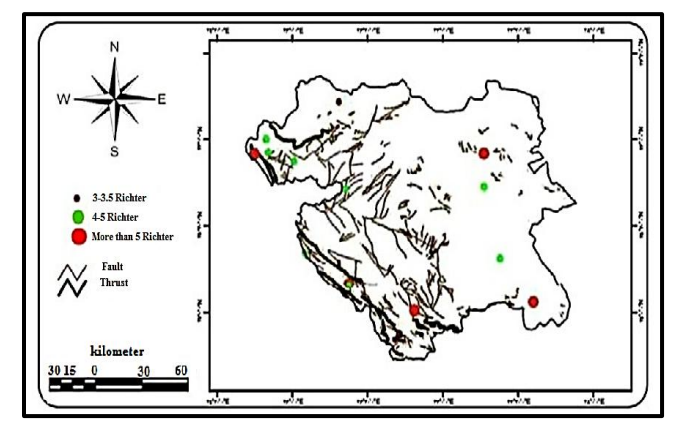


Fig. 5. Location map of faults in Kurdistan province (Malaki 2006) [8]

H.1.Lithology

The study of seismic centers and the study of the distribution of these units on the surface as the density of earthquake occurrences in Kurdistan Province shows that 23.6% of the area of the province is in the dense area and 30% of the area of the province is in the area with less density in terms of An earthquake has occurred, and the rest of the province is located in an area with an average density of earthquake occurrences. The low-intensity earthquake is located in the northern and northeastern regions of the province.

According to Figure 6 Subsurface lithology in Kurdistan province is generally divided into eleven units, which include basalt, dolomite, gabbro, limestone, calcareous sand, phyllite, conglomerate, schist, sandstone,

and volcanic rocks. The southwestern part of the province is covered with shale and calcareous sand. In the northern part, basalt and conglomerate outcrops showed several meters of remaining hills. Clay formations are near the southeast and parts of the northwest. In the south of the city, shale and schist are found, under which the solid rock begins.

The southwest and northwest of the city are covered by clay-sand-shale formations to depths of 10, 17, and 18 meters, respectively. From the center to the north of the province, spatially, it covers an area with a width of 60–80 km and an average length of 30–40 km, with a subsurface lithology of mainly clay-sand and sandstone formations, under which the rock is solid. Located at a depth of 20 meters in the west of the province, clay-sand formations can be seen at depths below 10, 17, and 18 meters where hard rocks meet. The rest of the province is covered by layers of sand up to 20 meters high. There are also volcanic rocks in the north and northeast of the province and along its east coast.

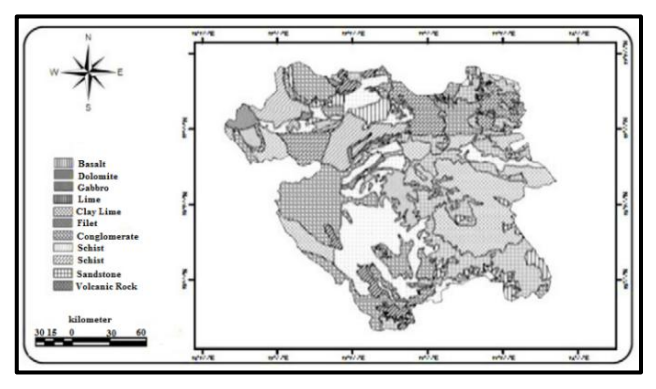


Fig. 6. Lithology map of Kurdistan Province (Malaki 2006) [8]

H.2.Geomorphology

Figure 7 shows the different cities of Kurdistan province according to their contribution to earthquake risk zoning. The soil surface texture map of Kurdistan province was prepared using soil profile data from the FAO

database. This information includes three layers (percentage of silt, clay and sand) along with the soil texture layer. Using the soil texture triangle, it is classified based on the United States Department of Agriculture (USDA) classification and is divided into 11 main soil texture classes in the Kurdistan region, which is shown in Figure 8. These statistics will enhance our view of the region for further analysis and more rational engineering prediction.

The results of the researchers' research are shown in a bar chart for each city, according to the percentage of the area of Kurdistan Province in earthquake risk zoning and the spatial distribution of surface soils of the region's geomorphological units, which can help in engineering perspective and final results. Also, according to Table 4, the earthquake risk rating is shown, which can ultimately be verified with the results obtained from the article and reach logical conclusions.

TABLE 4. EARTHQUAKE RISK GRADING IN THE CITIES OF KURDISTAN PROVINCE WITH GIS (MALAKI 2006) [8]

City name	The relative risk of an earthquake							
City name	Very Much	Much	Moderate	Low				
Baneh	*							
Bijar				*				
Saqqez			*					
Sanandaj		*						
Ghorveh			*					
Kamyaran			*					
Marivan	*							
Divandarreh			*					

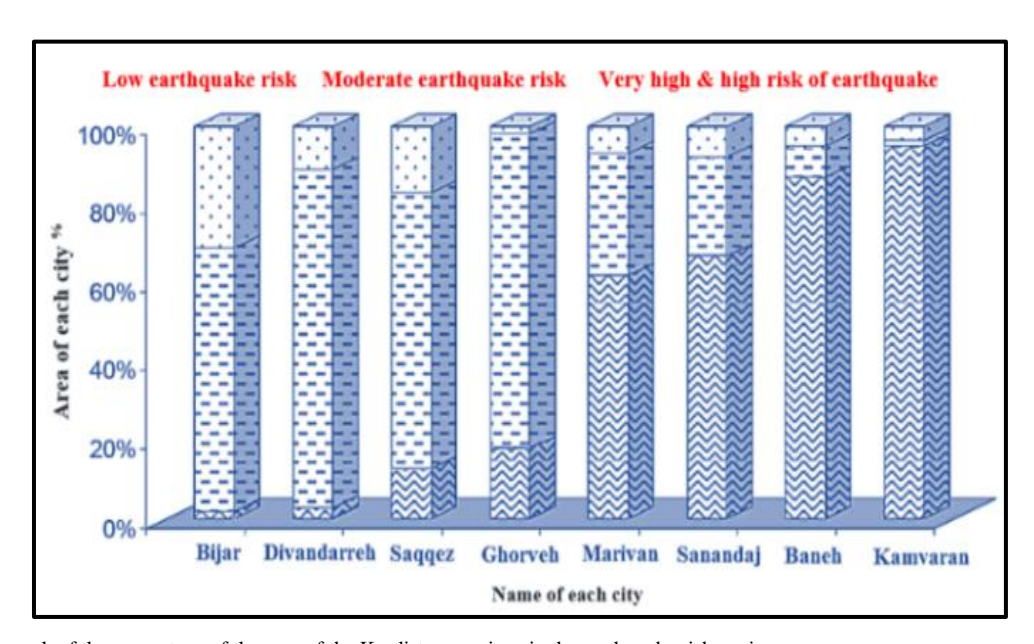


Figure 7. The graph of the percentage of the area of the Kurdistan province in the earthquake risk zoning

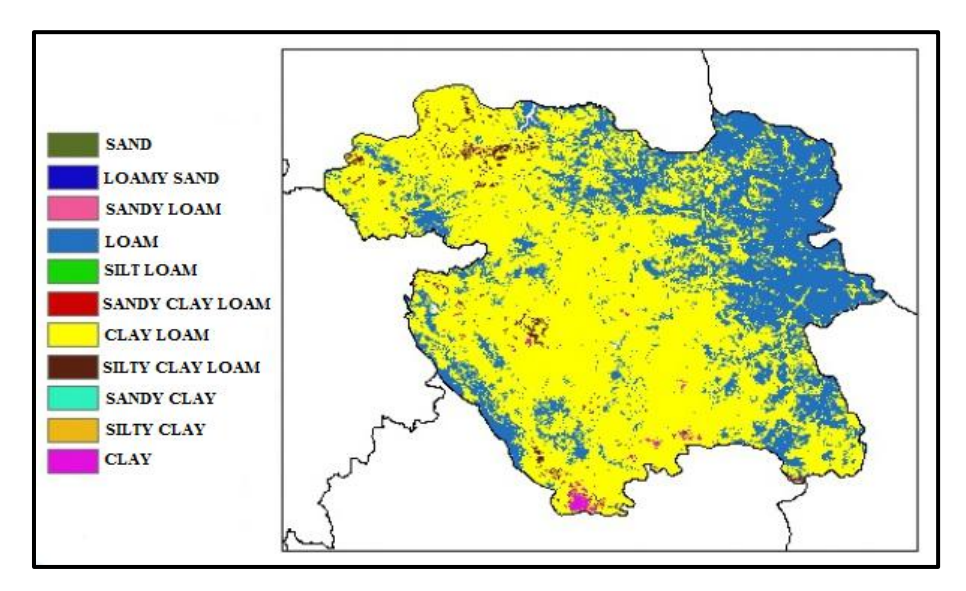


Figure 8. Spatial distribution surface soils of geomorphological units of Kurdistan

The classification of Iran's faults into active and inactive categories, along with associated reactivation probabilities, aligns with studies on seismicity patterns and fault behavior. Faults are categorized by length: main faults (>10 km), medium faults (2-10 km), and minor faults (<2 km). The Piranshahr fault, a critical seismic source, spans over 100 km in a northwest-southeast orientation and extends toward Saqqez, reflecting its role in regional tectonics. Its significance is further supported by historical seismic activity, such as reverse faulting events documented in Iran .The Santeh fault, oriented northeast-southwest and spanning ~50 km near Saqqez, exhibits visible fragmentation along the Divandre-Santeh road, indicating past tectonic activity. However, limited data on its age and seismicity highlight challenges in assessing reactivation risks, consistent with broader uncertainties in modeling inactive fault systems .Near the Velikhan River, a west-east trending fault connects to the Saqqez River system [32]. Such structural linkages are critical to regional tectonic lineaments, which influence seismic hazards and resource distribution .This framework integrates probabilistic models for fault activation and emphasizes the need for advanced like deep learning to differentiate active/inactive phases, particularly for poorly studied faults like Santeh. Further research is warranted to refine reactivation predictions and mitigate seismic risks.

According to seismographic data, the frequency of earthquakes with a magnitude of 3.5 on the Richter scale is higher in Saqqez city. These earthquakes typically have a shallow focal depth, ranging between 30–40 kilometers, which aligns with the seismic characteristics observed in the northwest region of the country. Most of the faults in this area are concentrated in the western and northwestern parts of Saqqez city. The horizontal expansion of the city has increased its proximity to these fault lines, thereby raising the likelihood of seismic impact and enhancing the city's vulnerability.

Furthermore, based on historical seismic maps and records, Saqqez city experiences earthquakes with magnitudes of 3 or greater on the Richter scale, as

categorized by the Hamelzer classification system. The earthquake risk levels in the region can be classified as follows:

- -Low Risk: Earthquakes with magnitudes less than 2 on the Richter scale.
- -Relatively Low Risk: Earthquakes with magnitudes between 2 and 3 on the Richter scale.
- -Moderate Risk: Earthquakes with magnitudes between 3 and 4 on the Richter scale.
- -High Risk : Earthquakes with magnitudes between 4 and 6 on the Richter scale.
- -Very High Risk: Earthquakes with magnitudes greater than 6 on the Richter scale.

Risk zoning within different areas of Saqqez city varies depending on the local geological conditions, environmental factors, and the degree of vulnerability to seismic activity. This zoning helps in assessing and managing the potential impacts of earthquakes across the region.

The image provided is a detailed log of a typical borehole in the Sagqez zone, focusing on its geomorphology. The log includes various parameters and observations recorded at different depths.

This log provides comprehensive data for understanding the subsurface geology and soil properties in the Sagqez zone, which is crucial for engineering and geological studies.

In Tables 5-7, according to the borehole test and also the fault details such as the fault length in the city of Saqqez, the geomorphology of this city can be used to give us a very excellent engineering view for liquefaction potential calculations, and finally the liquefaction potential in all cities of the province will be examined to obtain a general understanding of this area. Also, researchers in the future can conduct more extensive research in the field of liquefaction according to these results and provide technical solutions.

SPT N Value Symbol Depth " Blow Per 30 Depth ' Date Rock/Soil Description N Diagram 40 60 25/July/1401 Clay Loam ß 3.50 Sand and gravel and 3^m 4^m 5^m 6^m some organic debris Clay Loam Sand 4.0 5.0 " 8.5 5.45 " Moist, brown to grey 8 26/July/1401 ø sandy silt with 9^m 10.0 ° 9.0 " embedded gravel 11ª 10.45 12^m 38 oam 13^m 14.0 " 13.5 Medium to fine sand, 4 14ⁿ 27/July/1401 occasional clay lenses Clay 15ⁿ 14.45 " 14.0 Mottled brown and grey silty clay 16ⁿ Clay 2 18 17° 18ⁿ 18.0 ° 19ⁿ Compact, coarse to 28/July/140 ű, 18.45 20m medium sand and Shell 21.5 35 21^m fragments 22^m

TABLE 5. DETAILS OF A TYPICAL BOREHOLE IN THE SAQQEZ ZONE (GEOMORPHOLOGY)

Table 6. Characteristics of the faults of the whole province of $\,$ Kurdistan

Fault around all provinces	Fault Direction	Fault Length (L _F) ^{Km}	Faults Include
Fault north of Sanandaj	Northwest-Southeast	70	Main Faults
Kani Shah Fault	Northeast-Southwest	35	Main Faults
Santeh Fault	Northeast-Southwest	50	Main Faults
Northeast Fault of Baneh	Southwest-Northeast	40	Main Faults
Dinor Fault	The stretch of the west to the southeast	47	Main Faults
Morvarid Fault	Northwest-Southeast	22	Main Faults
Marivan Fault	135 degrees north-southwest	120	Main Faults

Table 7. Details of the faults of the whole city of $S\mbox{\sc aquez}$

Faults around the city of Saqqez	Fault Direction	Fault Length (L _F) ^{Km}	Faults Include
Piranshahr Fault	North-South	4.85	Medium Faults
Piranshahr Fault	South East	3.91	Medium Faults
Saqqez River	Northwest-Southeast	15.84	Main Faults
Santeh Fault	East West	7.9	Medium Faults
Santeh Fault	South-North	4.5	Medium Faults
Valikhan River	Southwest-Northeast	11.52	Main Faults

III. RESULTS AND DISCUSSION

Figures 9 and 10 compare the maximum liquefaction distance with earthquake magnitude for each of the faults in Kurdistan Province and the city of Saqez. The trend lines indicate that as earthquake magnitude increases, the maximum liquefaction distance also typically increases. However, there are variations among different studies, which may reflect differences in methodologies or interpretations of results. Ultimately, the results shown in these figures, which depict maximum liquefaction distances, are compared with tables derived from the lithology and geomorphology of Saqqez. The aim of this comparison is to establish a logical understanding of regional conditions and, in the future, enable the development of knowledge-based recommendations for strategies to mitigate liquefaction-induced damage.

The chart in Figure 9 compares the maximum liquefaction distance with the earthquake magnitude of

various faults in the entire province of Kurdistan. The x-axis represents the Earthquake Magnitude (M), while the y-axis shows the Maximum Liquefaction Distance (R) in kilometers.

Table 8 shows The lines connecting the data points for each model show the relationship between earthquake magnitude and maximum liquefaction distance. As the earthquake magnitude increases, the maximum liquefaction distance also tends to increase, though the exact relationship varies depending on the model used.

Tables 8 and 9 show the relationship between the maximum distance of the liquefaction zone and the magnitude created by each fault in Saqqez city and the entire Kurdistan province for a general understanding of the conditions in the region. Table 10 also compares the results of Saqqez city with the results of researchers.

TABLE 8. THE RELATIONSHIP BETWEEN THE MAXIMUM LIQUEFACTION DISTANCE WITH THE EARTHQUAKE MAGNITUDE OF EACH FAULT IN THE ENTIRE PROVINCE OF KURDISTAN

Faults around the city of Saqqez	Earthquake Magnitude (M _W)	Koribayashi and Tatsuoka (1975)	Ambrasey s (1977)	Seed et al. (1984)	Liu and Xie, (1984)	Tinsley (1985)	Wakamats u (1991)	Matsuoka (2015)
Fault north of Sanandaj	6.62	31.43	26.64	55.76	20.43	25.19	129.29	63.094
Kani Shah Fault	5.99	10.29	7.43	29.62	5.85	7.18	59.04	20.982
Santeh Fault	6.32	18.47	14.51	41.26	11.26	13.86	92.11	38.984
Northeast Fault of Baneh	6.11	12.73	9.48	33.42	7.42	9.12	70.13	26.624
Dinor Fault	6.26	16.60	12.85	38.85	10.00	12.30	85.49	35.106
Morvarid Fault	5.57	4.89	3.17	19.43	2.54	3.11	28.27	7.794
Marivan Fault	7.11	74.94	71.91	91.19	54.03	66.86	205.24	122.92

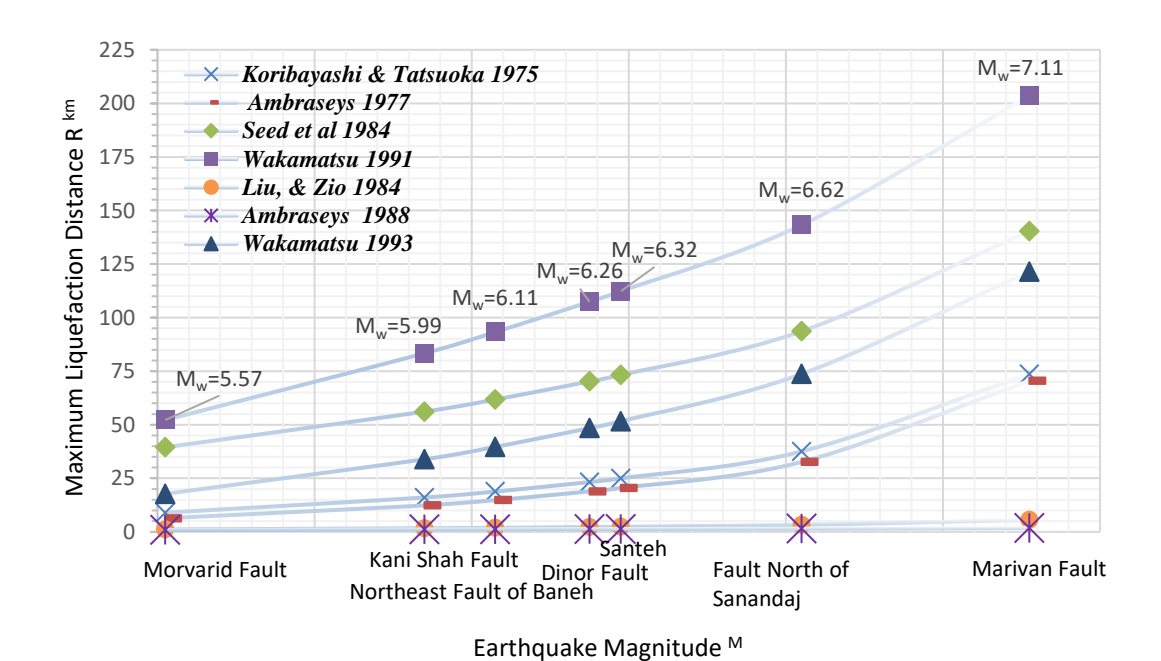


Figure 9. The chart Comparison the maximum liquefaction distance with the earthquake magnitude of each fault in the entire province of Kurdistan

TABLE 9. THE RELATIONSHIP BETWEEN THE MAXIMUM DISTANCE OF THE LIQUEFACTION ZONE AND THE MAGNITUDE CREATED BY EACH FAULT IN SAQQEZ CITY

Faults around the city of Saqqez	Earthquake Magnitude (M _W)	Koribayashi and Tatsuoka (1975)	Ambrasey s (1977)	Seed et al. (1984)	Liu and Xie, (1984)	Tinsley (1985)	Wakamats u (1991)	Matsuoka (2015)
Piranshahr Fault	4.44	0.66	0.32	6.25	0.27	0.33	-	0.005
Piranshahr Fault	4	0.30	0.13	4.02	0.11	0.14	-	-
Saqqez River	5.27	2.87	1.73	14.38	1.40	1.71	13.59	3.072
Santeh Fault	4.64	0.94	0.48	7.64	0.40	0.49	0.30	0.086
Santeh Fault	4.12	0.37	0.17	4.53	0.14	0.17	-	-
Valikhan River	4.98	1.72	0.96	10.75	0.79	0.96	4.74	0.905

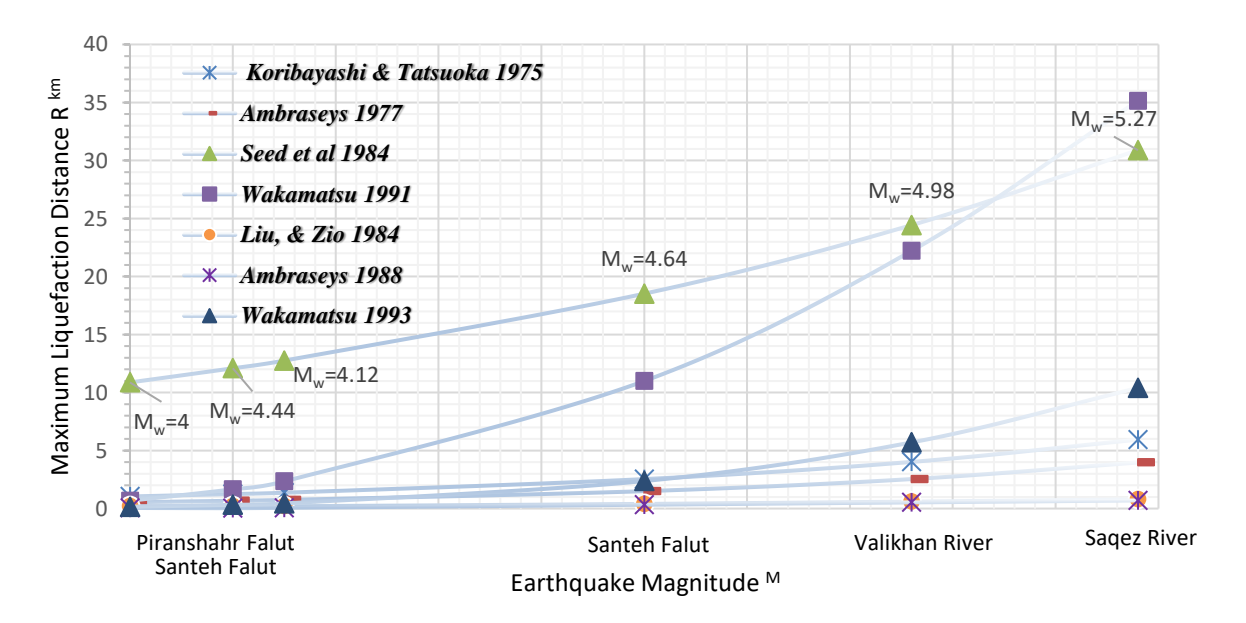


Figure 10. Chart comparing the maximum liquefaction distance with the earthquake magnitude of each fault in Saqqez city

Table 10 Comparison of the results obtained from research in the Saqqez River

Туре	Geomorphological unit	Classification
J.M.A(Wakamatsu 1992)	Dry river bed consisting of gravel	Not Likely
VIII ((unununu 1552)	Dry river bed consisting of sandy soil	Possibly
(Iwasaki 1982)	Present river bed, old river bed, swamp, reclaimed land, and inter-dune lowland	Liquefaction likely
Liquefaction of lithological	5 ^m –10.5 ^m -Sand Possible	
Equation of himotogram	17 ^m –22 ^m -Sand	Tossible
1-Distance of the Farthest Area with Liquefaction Potential to the Earthquake Focus (R), Mw=5.27	Seed et al.1984 and R=14.38 km	Liquefaction likely
2-Distance of the Farthest Area with Liquefaction Potential to the Earthquake Focus (R), Mw=4	Seed et al.1984 and R=4.02 $^{\rm km}$	Not Likely

The chart in Figure 10 compares the maximum liquefaction distance with the earthquake magnitude of each fault in Saqqez City. The x-axis represents the Earthquake Magnitude ($M_{\rm w}$), while the y-axis shows the Maximum Liquefaction Distance (R) in kilometers. Different studies are represented by various symbols and lines. The trend lines show that as the earthquake magnitude increases, the maximum liquefaction distance

also tends to increase. However, there is some variability among the different studies, indicating differences in methodologies or interpretations.

The geological and lithological sections of the Saqqez River were classified in different segments based on their susceptibility to liquefaction, considering specific ground motion conditions. Essential data for assessing and mitigating seismic hazards in various urban environments of Saqqez were identified. These results were further evaluated in light of the findings from previous studies. Ultimately, the findings obtained from this study were compared with the results derived from potential liquefaction hazard equations presented in Table 10

IV. LIQUEFACTION POTENTIAL HAZARDS OF KURDISTAN PROVINCE

Kurdistan province can be divided into two regions. eastern and western, in terms of seismicity. The western region includes the cities of Kamyaran, Sanandaj, Marivan, and Baneh, each of which has more than 55% of its area in the high-risk zone, and the eastern region includes the cities of Ghorveh, Bijar, Divandarreh, and Saggez, most of whose area is classified as moderate or low risk. In general, according to studies, 24% of the entire area of Kurdistan Province is in the high-risk area, and 78% is in the low-risk and moderate earthquake-risk area. The province can be divided into three parallel lines. That is, the western belt is in the zone with high risk, the central belt of the province is in the zone with moderate earthquake risk, and the eastern belt is in the zone with low earthquake risk. The province's relative number of earthquakes will decrease from south to north and from west to east. Evaluation of the liquefaction potential of the Kurdistan province Based on the lithology and geomorphological features, the city is divided into three areas: possible liquefaction, possible liquefaction, and the impossibility of liquefaction. Those areas are more prone to liquefaction. Such areas include hard rocks with sand and high-water tables. Young coastal plains and shallow alluvial plains are such landform units. The area where liquefaction is likely to occur is in northern.

Kurdistan. The geomorphological units of alluvial plains and older coastal plains in Kurdistan province are classified as liquefiable in the northwest and southeast. The southern part of Kurdistan and a patch of the northwestern part of the city fall under the "liquefaction is not likely" category. These areas are covered with solid rock, and there is no risk of liquefaction in the province.

The southern part of Kurdistan and a patch of the northwestern part of the city fall under the "liquefaction is not likely" category. However, current studies are based only on geological and geomorphic features. According to the results obtained from the methods available in the article, it can be seen that the potential of liquefaction in the Saqqez River is observed according to geomorphological and lithological methods, and that the probability of liquefaction in an earthquake between 3.5 and 4 on the Richter scale is not likely or possible. In the method of liquefaction risk zoning, if the magnitude of the

earthquake is between 3.5 and 4 according to the fault diagram of the city in the area of the Saqqez River, the probability of liquefaction is not likely according to the existing formulas. Also, if the probability of an earthquake according to the length of the fault is equal to 5 on the Richter scale, it can create a maximum of 35 km of liquefaction, and this magnitude of earthquake has a low probability in the studied area.

V. CONCLUSION

Based on the studies conducted in the studied area and zoning, the plains of this province have low to zero liquefaction potential, depending on the type and texture of deposits and the level of underground water. In other areas, due to the presence of stone structures and heights, there is no risk of liquefaction. Finally, the region into two possible and improbable areas in terms of the risk of liquefaction in the event of a future earthquake. The result is a map showing areas that are at risk of liquefaction in the future and should serve as a guide for further investigations into liquefaction potential. Since zoning can be considered the first level, its validation and refinement with more information is the task of future research.

Most commercial and industrial uses require studies in areas with high and medium liquefaction potential. These maps are useful for assessing the approximate areas affected by hazards and for disaster prevention planning, although the estimates are not detailed.

For structural engineers and geotechnical engineers, liquefaction hazard maps are essential to identify areas with liquefaction potential and consequences. The present studies can be a useful help for engineers, scientists, and planners as first-hand information for regional studies. Site-specific geotechnical investigations should be conducted in areas of high or moderate sensitivity to assess the risk to existing facilities and to assess and mitigate liquefaction risks before future development, especially when the area in question has significant socioeconomic benefits.

REFERENCES

- [1] Portahiri M, Ainali J, Ruknuddin R (2008) the role of capacity building in reducing Effects of natural hazards (earthquake) in rural areas with an emphasis on the quantitative method, Human Geography Research 74: 23-39
- [2] Bostani MD (1994) Review of the potential of soil psychiatrization in a region of the south and southwest. Master's Thesis, School of Civil Engineering. Tarbiat Modares University (in Persion).
- [3] Farzaneh O (1996) Studying the liquefaction potential of sandy soils in the Babolsar region. Master's Thesis, Civil Engineering, the University of Tehran (in Persian).
- [4] Hosseini MM, Arefpour S, Ghasemi A (1997) Manual of zonation on seismic geotechnical hazards, The Technical Committee for Earthquake Geotechnical Engineering, TC4 (in Persian).
- [5] Dewoolkar M, RYS Pak (2000) Experimental developments for studying walls with liquefiable backfills, Soil Dynamics and Earthquake Engineering 19:583-593.
- [6] Zamardian MJ (2002) Geomorphology of Iran. University Press Ferdowsi of Mashhad (in Persian).
- [7] Yamamoto K, Sugawara D (2003) Study on wall-type gravel drains as liquefaction countermeasure for underground structures, Soil Dynamics and Earthquake Engineering 23: 19-39.
- [8] Malaki A (2006) Earthquake risk zoning and prioritizing the improvement of province houses Kurdistan, Geographical Researches 59:124-115.
- [9] Ghanbari A, Saleki MA, Ghasemi M (2013) Vulnerability Zoning Cities against earthquake risk (case example: Tabriz city), Geography and Natural Hazards 5: 5-12.
- [10] Farajzadeh M, Basirat F (2006) Sensitivity Zoning of Geological Organizations against Shiraz Region Earthquake, Geographical Research 55: 59-72.

- [11] Ahdanjad RM (2010) Assessing the social vulnerability of cities against a sample earthquake in the case study of Zanjan city, Urban and regional studies and researches 7:71-90.
- [12] Karimi Z, Jafarizadeh A, Doulit A, Khairalhi H (2013) Risk Zone Earthquake in Qazvin province using geological data in the environment of the information Location system. The 32nd gathering and the first international congress of geoscience expertise (in Persian).
- [13] Ghadeiri M, Ruknuddin R, Parhizkar A, Shayan S (2009) an analysis of the theoretical perspectives of society's vulnerability to natural hazards, Modares Humanities Quarterly 1: 30-62.
- [14] Shia I, Habibi K, Torabi K (2010) Evaluation of the vulnerability of cities against earthquakes using the inverse hierarchy method and (GIS) case study of the 6th district of Tehran. 4th International Congress of Geographers of the Islamic World (in Persian).
- [15] Mandal P, Horton S (2007) Relocation of aftershocks, focal mechanisms, and stress inversion: Implications toward the seismotectonics of the causative fault zone of Mw 7.6 2001Bhuj earthquake (India), Tectonophys Journal. 429: 61–78.
- [16] Pase H (2009) Numerical study of liquefaction of alluvial foundations of earthen dams under earthquake loading. Civil Engineering, Master's Thesis, School of Civil Engineering, Tarbiat Modares University (in Persian).
- [17] Stein KH, Noralf R, Bjørg S, Lisbeth PD, Christer H (2007) Neotectonic faulting and the Late Weichselian shoreline gradients in SW Norway, Journal of Geodynamics 44: 96-128.
- [18] Zare M, Ghafory A, Mohsen B (1999) Attenuation law for the strong-motions in Iran, Proceedings of the Third International conference on seismology and Engineering, Tehran (in Persian).
- [19] Donald LW, Kevin JC (1994) New Empirical Relationships among Magnitude, Rupture Length, Rupture Width, Rupture Area, and Surface Displacement, Bulletin of the Seismological Society of America 84: 974-1002.
- [20] Kuribayashi E., Tatsuoka F. (1975) Brief review of liquefaction during earthquakes in Japan. Soils and found, The Japanese Society of Soil Mechanics and Foundation Engineering 15:81–92.
- [21] Matsuoka M, Wakamatsu K, Hashimoto M, Senna S and Midorikawa S (2015) Evaluation of liquefaction potential for large areas based on geomorphologic Classification, Earthquake Spectra 31: 2375–2395.
- [22] Seed HB, Tokimatsu K, Harder LF, & Chung RM (1985) The Influence of SPT Procedures in Soil Liquefaction Resistance Evaluations, Journal of Geotechnical Engineering 111: 1425-1445.
- [23] Liu Y, Xie JF (1984) Seismic liquefaction of sand, Earthquake Press China (in Chinese).
- [24] Tinsley JC, You'd TL, Perkins DM, Chen ATF (1985) Evaluating liquefaction potential, U.S. Geological Survey Professional Paper 1360 Washington DC.
- [25] Ambraseys NN (1977) Engineering Seismology, Earthquake Engineering, and Soil Dynamics 17: 1-15.
- [26] Wakamatsu, K (1991) Maps for historic liquefaction sites in Japan. Tokai University Press, Japan, 341pp. (in Japanese).
- [27] Matsuoka M, Wakamatsu K, Hashimoto M, Senna S and Midorikawa S (2015) Evaluation of liquefaction potential for large areas based on geomorphologic Classification, Earthquake Spectra 31: 2375–2395.
- [28] Iwasaki T, Tokida K, Tatsuoka F, Yasuda S, Sato H (1982) Micro zonation for soil liquefaction potential using simplified methods. Proc, 3rd Int. Conf. on Micro zonation, Seattle 3:1319-1330.
- [29] You'd TL, Perkins DM (1978) Mapping of liquefaction induced ground failure potential, Journal of Geotechnical Engineering Division 104: 433-446.
- [30] Stocklin J (1968) Structural history and tectonics of Iran, Bulletin of the American Association of Petroleum Geologists 52: 1229-1258.
- [31] Azizi H, Moinevaziri H (2009) Review of the tectonic setting of Cretaceous to Quaternary volcanism in northwest Iran, Journal of Geodynamics 47: 17-167.
- [32] Gandomi AH, Alavi AM (2012), A New Multi-Gene Genetic Programming Approach to Nonlinear System Modeling, Neural Computing and Applications 21: 171-187.